JAERI-M
88-004

NEANDC(J) 126/U
INDC(JPN) 112/L

EVALUATION OF NEUTRON NUCLEAR DATA FOR ^{252}CF AND ^{250}BK

February 1988

Tsuneo NAKAGAWA

日本原子力研究所
Japan Atomic Energy Research Institute

JAERI-M レポートは，日本原子力研究所が不定期に公刊している研究報告書です。
入手の問合わせは，日本原子力研究所技術情報部情報資料課（〒319-11茨城県那珂郡東海村）あて，お申しこしください。なお，このほかに財団法人原子力弘済会資料センター（〒319-11 茨城県那珂郡東海村日本原子力研究所内）で複写による実費頒布をおこなっております。

JAERI-M reports are issued irregularly.
Inquiries about availability of the reports should be addressed to Information Division Department of Technical Information, Japan Atomic Energy Research Institute, Tokai-mura, Naka-gun, Ibaraki-ken 319-11, Japan.

©Japan Atomic Energy Research Institute, 1988

編集兼発行　日本原子力研究所
印　　　刷　いばらき印刷㈱

JAERI-M 88-004

Evaluation of Neutron Nuclear Data for ^{252}Cf and ^{250}Bk

Tsuneo NAKAGAWA

Department of Physics
Tokai Research Establishment
Japan Atomic Energy Research Institute
Tokai-mura, Naka-gun, Ibaraki-ken

(Received January 6, 1988)

Neutron nuclear data of ^{252}Cf and ^{250}Bk have been evaluated in the neutron energy range from 10^{-5} eV to 20 MeV. The cross sections evaluated are the total, elastic and inelastic scattering, (n,2n), (n,3n), (n,4n) reaction, fission and capture cross sections. For the both nuclides, cross sections below 30 keV were represented with resolved and unresolved resonance parameters. For ^{252}Cf, the resolved resonance parameters were evaluated in the energy range from 10^{-5} eV to 1 keV and the unresolved resonance parameters above 1 keV. For ^{250}Bk, no resonance parameters have been reported. Therefore, hypothetical resolved resonance parameters were given below 100 eV. In addition, angular and energy distributions of emitted neutrons and average number of emitted neutrons per fission were also evaluated. Existing experimental data are only those for the fission cross section of ^{252}Cf, thermal cross sections and resonance integrals of ^{252}Cf and the fission cross section of ^{250}Bk at the thermal neutron energy. The present evaluation, therefore, was mainly based on the systematics of the data from neighboring nuclides and optical- and statistical-model calculations.

Keywords: Californium-252, Berkelium-250, Evaluation, Cross Section, Angular Distribution, Energy Distribution, Optical Model, Statistical Model

---

This work was performed under contracts between Power Reactor and Nuclear Fuel Development Corporation and Japan Atomic Energy Research Institute.

^{252}Cfと^{250}Bkの中性子核データの評価

日本原子力研究所東海研究所物理部
中川　庸雄

（1988年1月6日受理）

^{252}Cfと^{250}Bkの核データ評価を10^{-5}eVから20 MeV迄の中性子エネルギー範囲で行った。評価した断面積は，全断面積，弾性および非弾性散乱断面積，(n，2 n)，(n，3 n)，(n，4 n) 反応断面積，核分裂断面積，中性子捕獲断面積である。また，両方の核種とも30 keV以下は共鳴領域とし，^{252}Cfでは10^{-5}eVから1 keVの間を分離共鳴領域，それ以上を非分離共鳴領域とした。^{250}Bkについては，現在までに共鳴パラメータの測定値は，報告されていないが，100 eV以下を分離共鳴領域として仮想レベルを与え，それ以上を非分離共鳴領域とした。さらに，核反応後の放出中性子の角度分布データおよびエネルギー分布データや，核分裂当りの平均放出中性子数についても評価を行った。主な測定値は^{252}Cfの核分裂断面積，熱中性子エネルギー断面積および共鳴積分値，および^{250}Bkの熱中性子エネルギー核分裂断面積のみである。今回の評価は，前回までの評価と同様に，近傍核の核データの系統性，光学模型，統計模型などによる計算を利用して行い，これらの測定値と矛盾のない評価値を得た。

本報告書は，日本原子力研究所が動力炉・核燃料開発事業団の委託により行った研究の成果である。

Contents

1. Introduction 1
2. Evaluation for ^{252}Cf 1
2.1 Thermal Cross Sections and Resonance Integrals 1
2.2 Resonance Parameters 2
2.2.1 Resolved Resonance Parameters 2
2.2.2 Unresolved Resonance Parameters 3
2.3 Cross Sections above Resonance Region 4
2.3.1 Fission Cross Section 4
2.3.2 Level Density Parameters 4
2.3.3 (n,2n), (n,3n) and (n,4n) Reaction Cross Sections 4
2.3.4 Other Cross Sections 5
2.4 Other Quantities 5
2.4.1 Angular Distributions of Emitted Neutrons 5
2.4.2 Energy Distributions of Emitted Neutrons 5
2.4.3 Average Numbers of Neutrons Emitted per Fission 6
2.5 Comparison with Other Evaluation 7
3. Evaluation for ^{250}Bk 7
3.1 Resonance Parameters 7
3.1.1 Resolved Resonance Parameters 7
3.1.2 Unresolved Resonance Parameters 9
3.2 Cross Sections above Resonance Region 9
3.2.1 Fission Cross Section 9
3.2.2 Level Density Parameters 10
3.2.3 (n,2n), (n,3n) and (n,4n) Reaction Cross Sections 10
3.2.4 Other Cross Sections 10
3.3 Other Quantities 10
3.3.1 Angular Distributions of Emitted Neutrons 10
3.3.2 Energy Distributions of Emitted Neutrons 11
3.3.3 Average Numbers of Neutrons Emitted per Fission 11
4. Concluding Remarks 11
Acknowledgment 12
References 13

目　　次

1. 序　論 …… 1
2. ^{252}Cfの評価 …… 1
2.1 熱中性子断面積と共鳴積分値 …… 1
2.2 共鳴パラメータ …… 2
2.2.1 分離共鳴パラメータ …… 2
2.2.2 非分離共鳴パラメータ …… 3
2.3 共鳴領域より上の断面積 …… 4
2.3.1 核分裂断面積 …… 4
2.3.2 レベル密度パラメータ …… 4
2.3.3 (n，2n)，(n，3n)，(n，4n) 反応断面積 …… 4
2.3.4 その他の断面積 …… 5
2.4 その他の量 …… 5
2.4.1 放出中性子の角度分布 …… 5
2.4.2 放出中性子のエネルギー分布 …… 5
2.4.3 核分裂当たりの平均放出中性子数 …… 6
2.5 他の評価値との比較 …… 7
3. ^{250}Bkの評価 …… 7
3.1 共鳴パラメータ …… 7
3.1.1 分離共鳴パラメータ …… 7
3.1.2 非分離共鳴パラメータ …… 9
3.2 共鳴領域より上の断面積 …… 9
3.2.1 核分裂断面積 …… 9
3.2.2 レベル密度パラメータ …… 10
3.2.3 (n，2n)，(n，3n)，(n，4n) 反応断面積 …… 10
3.2.4 その他の断面積 …… 10
3.3 その他の量 …… 10
3.3.1 放出中性子の角度分布 …… 10
3.3.2 放出中性子のエネルギー分布 …… 11
3.3.3 核分裂当たりの平均放出中性子数 …… 11
4. 結　論 …… 11
謝　辞 …… 12
参考文献 …… 13

1. Introduction

For analysis of the higher actinide productions in the nuclear fuel cycle, reliable nuclear data of heavy nuclides are needed. The evaluation work on the neutron nuclear data of transplutonium isotopes has been performed under contracts between Power Reactor and Nuclear Fuel Development Corporation and Japan Atomic Energy Research Institute. So far, the data of sixteen nuclides from ^{241}Am to ^{251}Cf were evaluated and compiled in the ENDF format[1-14]. On this connection, the neutron nuclear data of ^{250}Bk and ^{252}Cf were evaluated in the present work.

The nuclide of ^{250}Bk has the half-life of 3.22 h for the β-decay. On the other hand, ^{252}Cf decays through 96.91 % of α-decay and 3.09 % of spontaneous fission with the half-life of 2.64 years. Only a few experiments on their cross sections have been made. Evaluated data are existing in ENDF/B-V[15] and ENDL-84[16] for ^{252}Cf and no evaluated data for ^{250}Bk.

The present evaluation work on ^{252}Cf is described in Section 2, and that on ^{250}Bk in Section 3. The evaluated quantities are summarized in Table 1.

2. Evaluation for ^{252}Cf

2.1 Thermal Cross Sections and Resonance Integrals

Experiments of the thermal cross sections of ^{252}Cf were summarized in Table 2. Halperin et al.[17] measured the capture cross section by using Oak Ridge Research Reactor. Their result of 20.4 ± 2 barns is consistent with the old measurement by Magnusson et al.[18] Harperin et al.[19] also carried out the experiment for the fission cross section with the method of solid-state track recording by using also the Oak Ridge Research Reactor. These cross sections of two reactions measured at ORNL are quite different from those by Folger et al.[20] and by Ruche[21], but in agreement with the absorption cross section measured by Anufriev et al.[22] In the present work, therefore, measurements at ORNL were adopted for the both reactions.

Table 3 shows the resonance integrals measured by four experiments performed so far. The value of Folger et al. might be too small.

Therefore, adopted are the capture resonance integral of 43.5 barns and the fission resonance integral of 110 barns both of which were measured at ORNL.

The thermal cross sections and resonance integrals thus adopted were used to determine the resonance parameters of low-lying levels. The finally recommended values in the present evaluation are the calculated values in Tables 2 and 3.

2.2 Resonance Parameters

2.2.1 Resolved Resonance Parameters

Moore et al.[23] measured the fission cross section of ^{252}Cf in the energy range from 20 eV to 5 MeV, using neutrons from the Physics-8 underground nuclear explosion, and obtained the sub-threshold fission areas for 35 resonances below 1 keV.

In the present evaluation, resonance parameters were determined for the 35 resonances from the fission-area data measured by Moore et al. by assuming an average fission width of 0.035 eV and an average radiative capture width of 0.035 eV. For some resonances, the minimum values of fission width were estimated by Moore et al. In such cases, those values were adopted as their fission width. From these 35 resonances, very small values of 0.634 barns for the capture cross section and 1.405 barns for the fission cross section are calculated at 0.0253 eV, respectively. Therefore, hypothetical levels were needed below 20 eV to reproduce the above-mentioned thermal cross sections.

Figure 1 shows staircase plot of total number of the measured resonances. From this figure it is seen that no significant level missing exists in the energy range from 20 eV to 1 keV, and average level spacing is 27.0 eV. Moore et al. obtained the s-wave strength function of 0.6×10^{-4} from the resonances below 500 eV. The parameters of hypothetical resonances were estimated on the basis of these average characteristics of resonance parameters. Then they were modified to reproduce above-mentioned values of thermal cross sections and resonance integrals. In the present evaluation, two resonances, one of which is located at negative energy and another above thermal neutron energy, were assumed. The resonance parameters including those of two hypothetical levels are listed in Table 4.

The effective scattering radius was determined from the shape elastic scattering cross section of 10.7 barns calculated with optical model parameters described below. The multilevel Breit-Wigner formula was applied to avoid negative elastic scattering cross sections. The resolved resonance region was connected to the unresolved resonance region at 1 keV.

Comparison of calculated fission cross section with Moore et al.'s experimental data is given in Fig. 2. Thermal cross sections and resonance integrals are compared in Tables 2 and 3, respectively. The present values calculated from the resonance parameters are in good agreement with the experimental data, except the capture resonance integral which is somewhat larger than the data of Halperin et al.

2.2.2 Unresolved Resonance Parameters

In the energy range from 1 to 30 keV, unresolved resonance parameters were determined with ASREP[25] so that calculated cross sections might be in good agreement with average fission cross section of Moore et al.'s data and capture cross section calculated with optical and statistical models. Adjusted parameters were the s-wave strength function, fission width and effective scattering radius. The p-wave strength function, average radiative width and D_{obs} were fixed to 3.37×10^{-4}, 35 meV and 27 eV, respectively. However, complete fit could not be obtained by this parameter search. Finally, small background cross sections were given in the energy range from 2.5 keV to 30 keV. Thus obtained unresolved resonance parameters are listed in Table 5. Figures 3 and 4 are comparison of fission and capture cross sections in the unresolved resonance region. Circles with error bar and dushed curve are cross sections to be reproduced. A solid curve shows the values calculated from the unresolved resonance parameters. Histogram below 1 keV is average values calculated from the resolved resonance parameters.

2.3 Cross Sections above Resonance Region

2.3.1 Fission Cross Section

The fission cross section was evaluated on the basis of the experimental data of Moore et al.[23] Below 10 keV, some fine structures exist in the cross-section shape. However, they were averaged over in suitable energy intervals and connected smoothly. In the energy range from 10 keV to 5 MeV, the experimental data were smoothed with spline functions. Above 5 MeV, cross section was estimated rather arbitrarily. Adopted fission cross section is shown in Fig. 5 together with Moore et al.'s experimental data and evaluated data in the ENDF/B-V[15].

Fomushkin et al.[26] measured the fission cross section of ^{252}Cf with a fast reactor neutron spectrum, and obtained the effective cross section of 1.58 ± 0.14 barns. They concluded that their result was in agreement with Moore et al.'s data within the experimental error.

2.3.2 Level Density Parameters

Level density parameters used are shown in Table 6. They were determined on the basis of Gilbert and Cameron's composite formula[27] by using the program LEVDENS[28], and adopting level schemes in ENSDF[29].

Pairing energies and shell corrections were taken from the values given by Gilbert and Cameron. Spin-cutoff factor was assumed to be

$$\sigma_M^2 = 0.146\ \sqrt{aU}\ A^{2/3} = \alpha_M\ \sqrt{U}\ .$$

2.3.3 (n,2n), (n,3n) and (n,4n) Reaction Cross Sections

The Q-values of the (n,2n), (n,3n) and (n,4n) reactions given in Table 7 were obtained from the compilation by Wapstra and Bcs[30]. Cross sections of these reactions were calculated with the evaporation model. The neutron emission cross section was assumed to be nearly equal to the difference between the compound nucleus formation cross section calculated with the optical model and the fission cross section mentioned above. In this calculation small value of 10 mb was assumed to be shared by the inelastic scattering cross section at high energies.

2.3.4 Other Cross Sections

The total, elastic, inelastic scattering and radiative capture cross sections were calculated with the program CASTHY[31] based on the spherical optical model and statistical model. The optical potential parameters shown in Table 8 were obtained by Igarasi and Nakagawa[7] so as to reproduce the total cross section of ^{241}Am measured by Phillips and Howe[32]. This set of optical potential parameters has been frequently used in our evaluation work for higher actinide data.

In the calculation, competition with the (n,2n), (n,3n), (n,4n) and fission reactions were taken into account. For the capture cross section, the average radiative width of 0.035 eV and s-wave level spacing of 27 eV were assumed.

Discrete level scheme of ^{252}Cf was taken from Nuclear Data Sheets[33]. The levels adopted for calculation of the inelastic scattering cross sections are given in Table 9. The levels above 1.03 MeV were considered to be overlapping.

Thus obtained cross sections in the energy range from 1 keV to 20 MeV are shown in Fig. 6. The total, fission and radiative capture cross sections in whole energy range are shown in Fig. 7.

2.4 Other Quantities

2.4.1 Angular Distributions of Emitted Neutrons

The angular distributions of elastically and inelastically scattered neutrons were calculated with the optical and statistical models. The isotropic distributions in the laboratory system were assumed for the inelastic scattering to the overlapping levels, and for the emitted neutrons from the (n,2n), (n,3n), (n,4n) and fission reactions.

2.4.2 Energy Distributions of Emitted Neutrons

The evaporation spectrum was assumed for the inelastically scattered neutrons (MT=91). The nuclear temperature θ was determined as

$$\theta = T, \qquad \text{for} \quad E_n \leq E_x, \qquad (1)$$

$$\theta = \{1+\sqrt{1+4a(E_n-\Delta)}\}/2a, \qquad \text{for} \quad E_n > E_x, \qquad (2)$$

where E_n is the incident neutron energy, and a and Δ are the level density parameter and the pairing energy of the residual nucleus. The parameter T is the nuclear temperature defined in the constant temperature model, and E_x is the energy where the constant temperature model is connected to the Fermi gas model. The neutron spectra from the (n,2n), (n,3n) and (n,4n) reactions were also represented with the evaporation model.

The Maxwellian spectrum was adopted for the fission neutrons. The temperature for the fission spectrum was determined from the systematics obtained by Smith et al.[34]

2.4.3 Average Numbers of Neutrons Emitted per Fission

(a) Prompt neutrons

Howerton's semi-empirical formula[35,36] was used for estimation of the average number of neutrons emitted per neutron-induced fission. His formula is in the following form for the target nucleus with the mass number of A and the atomic number of Z.

$$\nu(Z,A,E_n) = 2.33 + 0.06[2-(-1)^{A+1-Z}-(-1)^{Z}] + 0.15(Z-92) + 0.02(A-235) + [0.130+0.006(A-235)]\times[E_n-E_{th}(Z,A)] \quad (3)$$

where E_n is the incident neutron energy and the fission threshold energy E_{th} is written as follows.

$$E_{th}(Z,A) = 18.6 - 0.36Z^2/(A+1) + 0.2[2-(-1)^{A+1-Z}-(-1)^{Z}] - B_n. \quad (4)$$

where B_n stands for the neutron separation energy from compound nuclide. This formula predicts ν_p for ^{252}Cf as;

$$\nu_p = 3.884 + 0.230E_n. \quad (5)$$

(b) Delayed neutrons

The following systematics on the number of delayed neutrons was obtained by Tuttle[37]:

$$\nu_d = \exp[13.81+0.1754(A_c-3Z)(A_c/Z)] \quad (6)$$

where A_c is the mass number of the compound nucleus. We assumed that since the (n,n'f) channel opens around 7 MeV, the (n,n'f) process is always dominant above 7 MeV. The values of ν_d at lower energies and at higher energies were linearly connected between 6 and 8 MeV.

$$\nu_d = 0.00830\ (E_n<6\ \text{MeV}) \quad \text{and} \quad 0.00590\ (E_n>8\ \text{MeV}) \qquad (7)$$

2.5 Comparison with Other Evaluation

Evaluated data of ^{252}Cf are existing in ENDF/B-V[15] and ENDL-84[16]. The present results are compared with them in Figs. 8 to 12.

The evaluations for ENDF/B-V and ENDL-84 give resonance structure in the low energy region. In order to simplify the figures, cross sections in the resolved resonance region are averaged in 1/4-lethergy intervals.

In the energy range above 10 keV, Howerton's evaluation[16] was adopted in the both of ENDF/B-V and ENDL-84. In the lower energy range, the both evaluations adopted hypothetically generated resonance parameters. On the other hand, the present evaluation adopted mainly Moore et al.'s experimental data. Therefore, large discrepancies are found in this energy range. At the thermal energies, adopted cross sections in ENDF/B-V and the present evaluation are almost the same.

3. Evaluation for ^{250}Bk

3.1 Resonance Parameters

3.1.1 Resolved Resonance Parameters

Thermal fission cross section of 960 ± 150 barns was measured by Diamond et al.[38] And the capture cross section was assumed about 350 barns by Bol'shov et al.[39] These values are recommended by Mughabghab.[24] The present evaluation also adopted them.

No measurement has been made for the resonance parameters of ^{250}Bk so far. Therefore, the hypothetical resonance parameters were generated so as to reproduce the thermal cross sections. The s-wave strength function was assumed to be 0.83×10^{-4} which was calculated with the optical model. Average level spacing of 2.09 eV was derived from the level density parameter a of 30.0 MeV^{-1}. The effective scattering radius of 9.26 fm was obtained from the shape elastic scattering cross section calculated with the optical model. The average radiative width was assumed to be 0.035 eV. The fission width was estimated as 0.095 eV by assuming that the ratio of radiative and fission widths was equal to that of thermal cross sections.

Prince[40] derived the systematics of thermal cross sections and capture resonance integrals vs (B_n-E_f), where B_n is a binding energy and E_f is a fission threshold energy calculated as follows,

$$E_f = -106.247 + 12.99026(Z^2/A) - 0.438185(Z^2/A)^2 + 0.0045383(Z^2/A)^3 + \varepsilon \qquad (8)$$

where $\varepsilon = 0.0$ for even-even nuclides,
$\varepsilon = 0.47$ for odd mass nuclides,
$\varepsilon = 0.72$ for oad-odd nuclides.

In the case of ^{250}Bk, the value of (B_n-E_f) is 1.053, and from his systematics the following values are obtained.

$$\text{In}(I_r/2) = 5.3$$

$$\therefore I_r = 400 \text{ barns.} \qquad (9)$$

and

$$\text{In}(\sigma_f/\sigma_\gamma) = 0.5$$

$$\therefore \frac{\sigma_f}{\sigma_\gamma} = \frac{I_f}{I_\gamma} = \;\; 6$$

$$\therefore I_f = 660 \text{ barns.} \qquad (10)$$

The hypothetical resonances were generated by using above information. The energy of the first resonance was adjusted to roughly reproduce the thermal cross sections and resonance integrals. Then, only the energy of a negative resonance was re-adjusted on the basis of the thermal cross sections.

Thus obtained hypothetical resonance parameters reproduce well the thermal cross sections; the capture cross section of 353 barns and the fission cross section of 959 barns. The calculated resonance integrals are 199 barns and 517 barns for the radiative capture and fission cross sections, respectively. These values are smaller than the values estimated from Prince's systematics. No more adjustment, however, was tried because the estimated cross sections were not so accurate.

3.1.2 Unresolved Resonance Parameters

In the energy range from 100 eV to 30 keV, unresolved resonance parameters were determined with ASREP[25] in the same way as ^{252}Cf. The obtained unresolved resonance parameters are listed in Table 10.

3.2 Cross Sections above Resonance Region

3.2.1 Fission Cross Section

The shape of the fission cross section was assumed to be the same as that of ^{251}Cf[14], because the ^{251}Cf is also the nuclide with odd number of neutrons and the nearest one. As to the magnitude of the cross section, the following systematics obtained by Lasijo[41] was used to determine the value at 3 MeV.

$$\sigma_f = F(Z) + C\times[N-G(Z)]^2, \qquad (11)$$

where Z is the atomic number and N the neutron number, and F(Z) and G(Z) are given as

$$G(Z) = a_0 + a_1 Z + a_2 Z^2, \qquad (12)$$

a_0 = -2690.37063,
a_1 = 59.7373309,
a_2 = -0.3138082 ,

$$F(Z) = b_0 + b_1 Z + b_2 Z^2 + b_3 Z^3, \qquad (13)$$

b_0 = 2815.607814,
b_1 = -89.65620409,
b_2 = 0.94850607,
b_3 = -0.00333247,

and the constant C is 0.01702407. Based on this systematics, the cross-section shape was normalized to 2.03 barns at 3 MeV.

3.2.2 Level Density Parameters

Level density parameters of berkelium isotopes were determined with LEVDENS[28] on the basis of staircase plot of low-lying excited levels taken from ENSDF[29], and are shown in Table 11.

3.2.3 (n,2n), (n,3n) and (n,4n) Reaction Cross Sections

The Q-values of the (n,2n), (n,3n) and (n,4n) reactions are given in Table 12.

These cross sections were calculated with the same method as ^{252}Cf.

3.2.4 Other Cross Sections

The total, elastic, inelastic scattering and radiative capture cross sections were calculated with CASTHY based on the spherical optical model and statistical model by using the optical potential parameters shown in Table 8.

For the capture cross section, the average radiative width of 0.035 eV and s-wave level spacing of 2.09 eV were adopted.

Discrete level scheme was taken from Nuclear Data Sheets[33]. The levels adopted for calculation of the inelastic scattering cross sections are given in Table 13. The levels above 296 keV were considered to be overlapping.

Thus calculated cross sections in the energy range from 100 eV to 20 MeV are illustrated in Fig. 13. The total, fission and radiative capture cross sections in whole energy range are shown in Fig. 14.

3.3 Other Quantities

3.3.1 Angular Distributions of Emitted Neutrons

The angular distributions of elastically and inelastically scattered neutrons were calculated with the optical and statistical models. The isotropic distributions in the laboratory system were assumed for the inelastic scattering to the overlapping levels, and for the emitted neutrons from the (n,2n), (n,3n), (n,4n) and fission reactions.

3.3.2 Energy Distributions of Emitted Neutrons

Evaporation spectra were given for inelastically scattered neutrons (MT=91) and those from (n,2n), (n,3n) and (n,4n) reactions.

The Maxwellian spectrum was adopted for the fission neutrons. The temperature for the fission spectrum was determined from the systematics obtained by Smith et al.[34]

3.3.3 Average Numbers of Neutrons Emitted per Fission

(a) Prompt neutrons

Howerton's semi-empirical formula gives the following values.

$$\nu_p = 3.559 + 0.220E_n. \tag{14}$$

(b) Delayed neutrons

The values obtained from Tuttle's systematics are

$$\nu_d = 0.0130 \ (E_n<6 \text{ MeV}) \quad \text{and} \quad 0.0089 \ (E_n>8 \text{ MeV}) \tag{15}$$

4. Concluding Remarks

In the present work, the neutron nuclear data of ^{250}Bk and ^{252}Cf were evaluated, and compiled in the ENDF-5 format.

In the past several years, we evaluated neutron nuclear data for isotopes of Am, Cm, Bk and Cf. Table 14 lists the thermal cross sections and resonance integrals of these isotopes. The number of experimental data is very limited for those isotopes. The large part of data was, therefore, estimated with spherical optical model and statistical model, and also with systematics of the data.

The optical potential parameters were determined to reproduce the total cross section of ^{241}Am. This set of parameters was used for many isotopes even in the case of nuclides far from ^{241}Am. The reliability of the optical potential parameters should be checked. However, other experiments on total or elastic scattering cross section which can be used to check the parameters are not available for transplutonium isotopes so far.

Direct reactions and/or pre-equilibrium theory should be taken into account to calculate more accurately the inelastic scattering and (n,Xn) reaction cross sections at high energies. In our evaluation, these contributions have been ignored because the data in high energy region are not so important for nuclear fuel cycle. However, in the future, this defect must be improved.

In order to determine the reliable thermal cross sections and resonance integrals, the resonance parameters of low-lying levels are very important. For some isotopes, hypothetical levels were generated. These assumed resonances should be replaced with experimentally obtained data in the future.

Even if these problems are existing, a series of our evaluation work has prepared a reliable data base for the nuclear fuel cycle study.

Acknowledgment

The author thanks members of the Nuclear Data Center of JAERI for their help to the present work.

References

1) Igarasi S. : "Evaluation of ^{241}Am Nuclear Data", JAERI-M 6221 (1975) [in Japanese].
2) Igarasi S. : J. Nucl. Sci. Technol., 14, 1 (1977).
3) Nakagawa T., Fuketa T. and Igarasi S. : "Evaluation of the Neutron Data of ^{241}Am", JAERI-M 6636 (1976) [in Japanese].
4) Igarasi S. and Nakagawa T. : "Evaluation of Neutron Nuclear Data for ^{243}Am", JAERI-M 7174 (1977) [in Japanese].
5) Igarasi S. and Nakagawa T. : "Evaluation of Neutron Nuclear Data for ^{244}Cm", JAERI-M 7175 (1977) [in Japanese].
6) Igarasi S. and Nakagawa T. : "Evaluation of Neutron Nuclear Data for ^{245}Cm", JAERI-M 7733 (1978) [in Japanese].
7) Igarasi S. and Nakagawa T. : "Evaluation of Neutron Nuclear Data for ^{242}Cm", JAERI-M 8342 (1979) [in Japanese].
8) Nakagawa T. and Igarasi S. : "Evaluation of Neutron Nuclear Data for ^{242m}Am and ^{242g}Am", JAERI-M 8903 (1980).
9) Nakagawa T. and Igarasi S. : "Evaluation of Neutron Nuclear Data for ^{243}Cm", JAERI-M 9601 (1981).
10) Kikuchi Y. : "Evaluation of Neutron Nuclear Data for ^{241}Am and ^{243}Am", JAERI-M 82-096 (1982).
11) Kikuchi Y. : "Evaluation of Neutron Nuclear Data for ^{246}Cm and ^{247}Cm", JAERI-M 83-236 (1983).
12) Kikuchi Y. and Nakagawa T. : "Evaluation of Neutron Nuclear Data for ^{248}Cm and ^{249}Cm", JAERI-M 84-116 (1984).
13) Kikuchi Y. and Nakagawa T. : "Evaluation of Neutron Nuclear Data for ^{249}Bk and ^{249}Cf", JAERI-M 85-138 (1985).
14) Nakagawa T. : "Evaluation of Neutron Nuclear Data for ^{250}Cf and ^{251}Cf", JAERI-M 86-086 (1986).
15) ENDF/B-V MAT=8852, summary is given as England T.R., Wilson W.B., Schenter R.E. and Mann F.M. : "Summary of ENDF/B-V Data for Fission Products and Actinides", EPRI NP-3787 (also ENDF-322) (1984).
16) Howerton R.J. and MacGregor M.H. : "The LLL Evaluated Nuclear Data Library (ENDL): Descriptions of Individual Evaluations for Z=0-98", UCRL-50400, Vol.15, Part D., Rev.1 (1978).
17) Halperin J., Bemis C.E., Druschel R.E. and Stokely J.R. : Nucl. Sci. Eng., 37, 223 (1969).

18) Magnusson L.B., Studier M.H., Fields P.R., Stevens C.M., Mech J.F., Friedman A.M., Diamond H. and Huizenga J.R. : Phys. Rev., 96, 1576 (1954).

19) Halperin J., Oliver J.H. and Stroughton R.W. : "The Thermal Cross Section and Resonance Integral for Neutron Fission of ^{252}Cf", ORNL 4706, 51 (1971).

20) Folger R.L., Smith J.A., Brown L.C., Overman R.F. and Holcomb H.P. : Proc. of Conf. on Nucl. Cross Sections and Technol., Washington D.C., 4-7 March, 1968, NBS special publication 299, 1279 (1968).

21) Ruche B.C. : Trans. Amer. Nucl. Soc., 14, 344 (1971).

22) Anufriev V.A., Gavrilov V.D., Zamyatnin Yu.S. and Ivanenko V.V. : Sov. At. Energy, 36, 359 (1973).

23) Moore M.S., McNally J.H. and Baybarz R.D. : Phys. Rev., C 4, 273 (1971).

24) Mughabghab S.F. : "Neutron Cross Sections, Vol.1, Neutron Resonance Parameters and Thermal Cross Sections, Part B: Z=61-100", Academic Press (1984).

25) Kikuchi Y. : private communication.

26) Fomushkin E.F., Gutnikova E.K., Novoselov G.F. and Panin V.I. : Sov. At. Energy, 40, 202 (1976).

27) Gilbert A. and Cameron A.G.W. : Can. J. Phys., 43, 1446 (1965).

28) Iijima S. : to be published as JAERI-M report.

29) ENSDF : Evaluated Nuclear Structure Data File.

30) Wapstra A.H. and Bos K. : Atomic Data and Nucl. Data Tables, 19, No.3 (1977).

31) Igarasi S. : J. Nucl. Sci. Technol., 12, 67 (1975).

32) Phillips T.W. and Howe R.E. : Nucl. Sci. Eng., 69, 375 (1979).

33) Schmorak M.R. : Nucl. Data Sheets, 32, 87 (1981).

34) Smith A., Guenther P., Winkler G. and McKnight R. : "Prompt-Fission-Neutron Spectra of ^{233}U, ^{235}U, ^{239}Pu and ^{240}Pu Relative to the That of ^{252}Cf", ANL/NDM-50 (1979).

35) Howerton R.J. : Nucl. Sci. Eng., 46, 42 (1971).

36) Howerton R.J. : Nucl. Sci. Eng., 62, 438 (1977).

37) Tuttle, R.J. : Proc. Consultants' Meeting on Delayed Neutron Properties, Vienna, 26-30 March 1979, INDC(NDS)-107/G+Special, 29 (1979).

38) Diamond H., Hines J.J. Sjoblom R.K., Barnes R.F., Metta D.N., Lerner J.L. and Fields P.R. : J. Inorg. Nucl. Chem., 30, 2553 (1968).

39) Bol'shov V.I., Dubinin A.A., Dmitriv V.M., Kapchigashev S.P., Kon'shin V.A., Matusevich E.S., Polivanskii V.P., Pupko V.Ya., Regushevskii V.I., Stavisskii Yu.Ya. and Yur'ev Yu.S. : Sov. At. Energy, 26, 497 (1970).

40) Prince A. : Proc. of Conf. on Nucl. Cross Sections and Technol., Washington D.C., 4-7 March, 1968, NBS special publication 299, 2, 951 (1968).

41) Lasijo R.S. : private communication (1986).

Table 1 Quantities evaluated in the present work

Quantities	Energy range Bk-250	Energy range Cf-252
1) Resonance parameters		
Resolved resonances	-0.24 - 116.8eV	-3.50 - 983.5eV
Resolved resonance region	10^{-5} - 100eV	10^{-5} - 1000eV
Unresolved resonance region	0.10 - 30.0keV	1.00 - 30.0keV
2) Cross sections		
Total	10^{-5}eV - 20MeV	10^{-5}eV - 20MeV
Elastic scattering	10^{-5}eV - 20MeV	10^{-5}eV - 20MeV
Inelastic scattering	34.14keV - 20MeV	45.90keV - 20MeV
Fission	10^{-5}eV - 20MeV	10^{-5}eV - 20MeV
Radiative capture	10^{-5}eV - 20MeV	10^{-5}eV - 20MeV
(n,2n)	4.990 - 20MeV	6.195 - 20MeV
(n,3n)	11.23 - 20MeV	11.33 - 20MeV
(n,4n)	16.82 - 20MeV	17.98 - 20MeV
3) Angular distributions of emitted neutrons		
Angular distributions of elastically and inelastically scattered neutrons, and those from (n,2n), (n,3n), (n,4n) and fission reactions were given in the same energy range as their cross-section data.		
4) Energy distributions of emitted neutrons		
Inelastic to continuum	0.2972 - 20MeV	1.034 - 20MeV
Fission	10^{-5}eV - 20MeV	10^{-5}eV - 20MeV
(n,2n)	4.990 - 20MeV	6.195 - 20MeV
(n,3n)	11.23 - 20MeV	11.33 - 20MeV
(n,4n)	16.82 - 20MeV	17.98 - 20MeV
5) Other quantities		
ν_d	10^{-5}eV - 20MeV	10^{-5}eV - 20MeV
ν_p	10^{-5}eV - 20MeV	10^{-5}eV - 20MeV

Table 2 Thermal cross sections of ^{252}Cf

(barns)

	capture	fission	absorption
Magnusson et al.[18]	25		
Folger et al.[20]			8.6
Ruche[21] (a)		0	19.8
(b)		6	28
Halperin et al.[17]	20.4±2		
Halperin et al.[19]		32±4	
Anufriev et al.[22]			63±9
Mughabghab[24]	20.4±1.5	32±4	
ENDF/B-V	20.6	32.3	
Calculated	20.07	33.03	

Table 3 Resonance integrals of ^{252}Cf

(barns)

	capture	fission	absorption
Folger et al.[20]			42
Ruche[21] (a)		0	44
(b)		12	58
Halperin et al.[17]	43.5±3		
Halperin et al.[19]		110±30	
Mughabghab[24]	43.5±1.5	110±30	
ENDF/B-V	47.4	120	
Calculated	47.4	111	

Table 4 Resonance parameters of ^{252}Cf

(barns)

energy(eV)	Γ_n(eV)	Γ_γ(eV)	Γ_f(eV)
-3.5000E+00	3.0500E-03	3.5000E-02	5.0000E-02
1.4000E+00	0.0192E-03	3.5000E-02	1.3000E-01
2.4550E+01	2.4197E-04	3.5000E-02	3.5000E-02
3.6350E+01	1.3117E-02	3.5000E-02	3.5000E-02
6.8370E+01	5.3500E-02	3.5000E-02	1.8000E-01
7.9160E+01	3.9871E-03	3.5000E-02	3.5000E-02
8.8250E+01	2.4978E-04	3.5000E-02	3.5000E-02
1.3810E+02	1.7060E-03	3.5000E-02	3.5000E-02
1.9010E+02	1.7918E-03	3.5000E-02	3.5000E-02
2.1770E+02	1.6000E-01	3.5000E-02	3.5000E-02
2.4620E+02	4.1870E-03	3.5000E-02	3.5000E-02
3.0710E+02	3.8936E-03	3.5000E-02	3.5000E-02
3.3800E+02	2.5024E-03	3.5000E-02	3.5000E-02
3.8740E+02	2.5774E-02	3.5000E-02	3.5000E-02
3.9360E+02	2.8690E-03	3.5000E-02	3.5000E-02
4.0480E+02	3.3027E-02	3.5000E-02	3.5000E-02
4.1700E+02	4.9036E-03	3.5000E-02	3.5000E-02
4.2670E+02	1.8327E-02	3.5000E-02	3.5000E-02
4.4540E+02	1.7284E-02	3.5000E-02	3.5000E-02
4.9080E+02	1.2025E-02	3.5000E-02	3.5000E-02
5.2020E+02	5.1604E-03	3.5000E-02	3.5000E-02
5.5720E+02	3.7000E-01	3.5000E-02	4.2500E-02
5.6190E+02	3.0641E-02	3.5000E-02	3.5000E-02
6.0640E+02	6.8026E-02	3.5000E-02	3.5000E-02
6.2640E+02	3.1845E-03	3.5000E-02	3.5000E-02
6.4370E+02	4.3202E-03	3.5000E-02	3.5000E-02
6.7420E+02	1.2340E-02	3.5000E-02	3.5000E-02
7.0620E+02	1.2555E-02	3.5000E-02	3.5000E-02
7.2610E+02	1.2500E+00	3.5000E-02	8.2000E-02
7.5410E+02	1.9146E-02	3.5000E-02	3.5000E-02
7.7110E+02	2.0948E-02	3.5000E-02	3.5000E-02
8.1350E+02	3.7509E-03	3.5000E-02	3.5000E-02
8.3310E+02	1.3000E+00	3.5000E-02	4.4000E-02
8.4100E+02	8.2260E-03	3.5000E-02	3.5000E-02
8.7760E+02	1.6312E-02	3.5000E-02	3.5000E-02
9.3180E+02	8.0871E-03	3.5000E-02	3.5000E-02
9.8350E+02	5.1330E-03	3.5000E-02	3.5000E-02

Table 5 Unresolved Resonance parameters of ^{252}Cf

energy (keV)	S_0 (10^{-4})	S_1 (10^{-4})	D-obs (eV)	Γ_f (eV)	Γ_γ (eV)
1.0	1.22	3.37	26.9	0.0565	0.035
1.25	1.22	3.37	26.9	0.0599	0.035
1.5	1.22	3.37	26.9	0.0625	0.035
1.75	1.22	3.37	26.9	0.0654	0.035
2.0	1.22	3.37	26.9	0.0666	0.035
2.5	1.22	3.37	26.8	0.0683	0.035
3.0	1.22	3.37	26.8	0.0700	0.035
4.0	1.22	3.37	26.7	0.0754	0.035
5.0	1.22	3.37	26.7	0.0760	0.035
6.0	1.22	3.37	26.6	0.0765	0.035
7.0	1.22	3.37	26.6	0.0773	0.035
8.0	1.22	3.37	26.5	0.0767	0.035
9.0	1.22	3.37	26.4	0.0778	0.035
10.0	1.22	3.37	26.4	0.0780	0.035
12.5	1.22	3.37	26.2	0.0799	0.035
15.0	1.22	3.37	26.1	0.0801	0.035
17.5	1.22	3.37	25.9	0.0818	0.035
20.0	1.22	3.37	25.8	0.0827	0.035
25.0	1.22	3.37	25.5	0.0893	0.035
30.0	1.22	3.37	25.2	0.0965	0.035

Table 6 Level density parameters of Californium isotopes

	Cf-249	Cf-250	Cf-251	Cf-252	Cf-253
a(MeV^{-1})	29.9	31.2	32.2	31.6	32.2
α_M($MeV^{-1/2}$)	31.60	32.36	32.97	32.74	33.14
Δ(MeV)	0.77	1.673	0.77	1.635	0.77
T(MeV)	0.3693	0.4025	0.3809	0.3927	0.3322
C(MeV)	5.416	2.093	14.84	1.895	3.59
E_x(MeV)	3.636	5.418	4.204	5.233	3.226

Table 7 Q-values and threshold energies of ^{252}Cf (n,Xn) reactions

reaction	Q-value (MeV)	E_{th} (MeV)
(n,2n)	-6.1707	6.1954
(n,3n)	-11.2822	11.3273
(n,4n)	-17.9057	17.9773

Table 8 Optical potential parameters

(MeV and fm)

$V = 43.4 - 0.107E_n$

$W_s = 6.95 - 0.339E_n + 0.0531E_n^2$

$V_{so} = 7.0$

$r_0 = r_{so} = 1.282$

$r_s = 1.29$

$a = a_{so} = 0.60$

$b = 0.5$

Table 9 Level scheme of ^{252}Cf

No.	Energy (keV)	spin-parity
ground	0.0	0 +
1	45.72	2 +
2	151.73	4 +
3	804.82	2 +
4	830.81	2 -
5	845.72	3 +
6	867.51	3 -
7	900.3	4 +
8	917.03	4 -
9	969.83	3 +

Levels above 1.03 MeV were assumed to be overlapping.

Table 10 Unresolved Resonance parameters of ^{250}Bk

energy (keV)	S_0 (10^{-4})	S_1 (10^{-4})	D-obs (eV)	Γ_f (eV)	Γ_γ (eV)
0.1	0.822	3.92	2.09	0.104	0.035
0.5	0.822	3.92	2.09	0.104	0.035
0.2	0.822	3.92	2.09	0.104	0.035
0.3	0.822	3.92	2.09	0.105	0.035
0.4	0.822	3.92	2.09	0.105	0.035
0.5	0.822	3.92	2.09	0.104	0.035
0.6	0.822	3.92	2.09	0.102	0.035
0.8	0.822	3.92	2.09	0.106	0.035
1.0	0.822	3.92	2.09	0.101	0.035
1.5	0.822	3.92	2.08	0.0998	0.035
2.0	0.822	3.92	2.08	0.104	0.035
3.0	0.822	3.92	2.08	0.108	0.035
4.0	0.822	3.92	2.07	0.118	0.035
5.0	0.822	3.92	2.07	0.120	0.035
6.0	0.822	3.92	2.06	0.123	0.035
7.0	0.822	3.92	2.06	0.127	0.035
8.0	0.822	3.92	2.06	0.134	0.035
10.0	0.822	3.92	2.05	0.139	0.035
12.5	0.822	3.92	2.04	0.146	0.035
15.0	0.822	3.92	2.03	0.155	0.035
20.0	0.822	3.92	2.01	0.168	0.035
25.0	0.822	3.92	1.98	0.190	0.035
30.0	0.822	3.92	1.96	0.208	0.035

Table 11 Level density parameters of Berkelium isotopes

	Bk-247	Bk-248	Bk-249	Bk-250	Bk-251
a(MeV^{-1})	28.1	27.8	34.2	30.05	30.0
α_M($MeV^{-1/2}$)	30.47	30.39	33.79	31.76	31.82
Δ(MeV)	0.39	0.0	0.903	0.0	0.865
T(MeV)	0.364	0.326	0.366	0.340	0.385
C(MeV)	2.90	10.8	12.2	24.6	6.56
E_x(MeV)	7.97	1.85	4.30	2.34	4.05

Table 12 Q-values and threshold energies of ^{250}Bk (n,Xn) reactions

reaction	Q-value (MeV)	E_{th} (MeV)
(n,2n)	-4.9697	4.9897
(n,3n)	-11.1834	11.2285
(n,4n)	-16.7491	16.8166

Table 13 Level scheme of ^{250}Bk

No.	Energy (keV)	spin-parity
ground	0.0	2 -
1	34.5	3 -
2	35.6	4 +
3	78.1	5 +
4	86.4	7 +
5	97	5 -
6	104.1	1 -
7	125.4	2 -
8	129	6 +
9	131.9	3 +
10	157	8 +
11	167	6 -
12	175.4	1 +
13	191	7 +
14	211.8	2 +
15	237	3 +
16	242	9 +
17	248	7 -
18	270	4 +

Levels above 296 keV were assumed to be overlapping.

Table 14 Thermal cross sections and resonance integrals of 18 nuclides

Nuclide	Thermal cross sections(b)		Resonanse integrals(b)	
	capture	fission	capture	fission
Am-241	600.3	3.02	1300	14.7
Am-242	5500	2100	390	1260
Am-242m	1342	6620	207	1530
Am-243	78.50	228.0	1820	11.4
Cm-242	15.92	5.00	116	11.1
Cm-243	131.3	512.3	404	1750
Cm-244	14.41	1.18	594	18.4
Cm-245	346.3	2001	108	799
Cm-246	1.33	0.142	103	9.5
Cm-247	59.9	97.0	495	769
Cm-248	2.57	0.37	257	17.5
Cm-249	1.60	0.82	215	139
Bk-249	709.6	3.96	1130	12.1
Bk-250	353	959	199	517
Cf-249	504.5	1666	695	2220
Cf-250	1779	4.09	8420	27.8
Cf-251	2878	4935	1610	2780
Cf-252	20.07	33.03	47.4	111

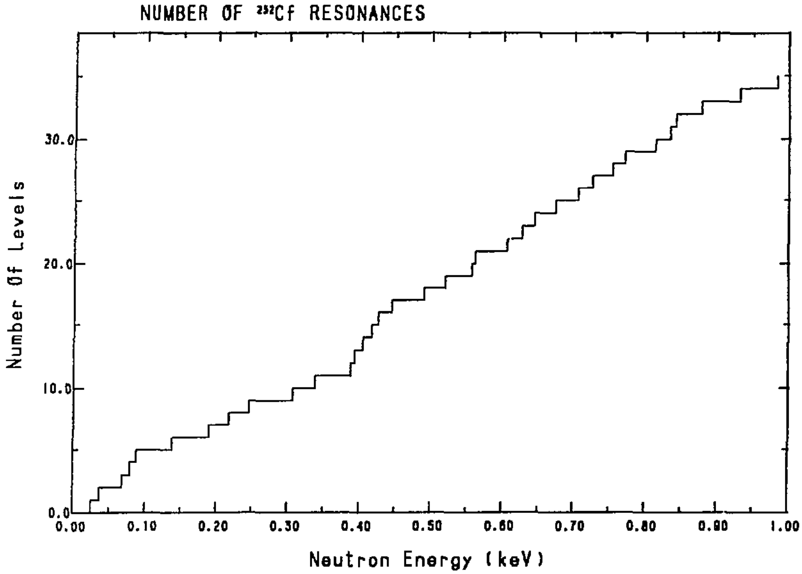

Fig. 1 Staircase plot of total number of ^{252}Cf resonances

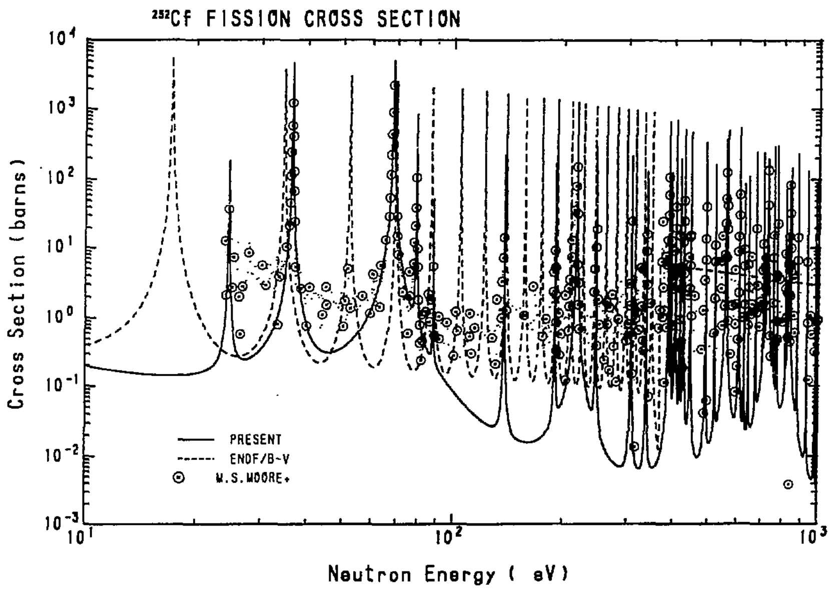

Fig. 2 Fission cross section in the energy range from 10 to 1000 eV. Solid curve is calculated values based on the present evaluation. Circles are the experimental data measured by of Moore et al. [23]

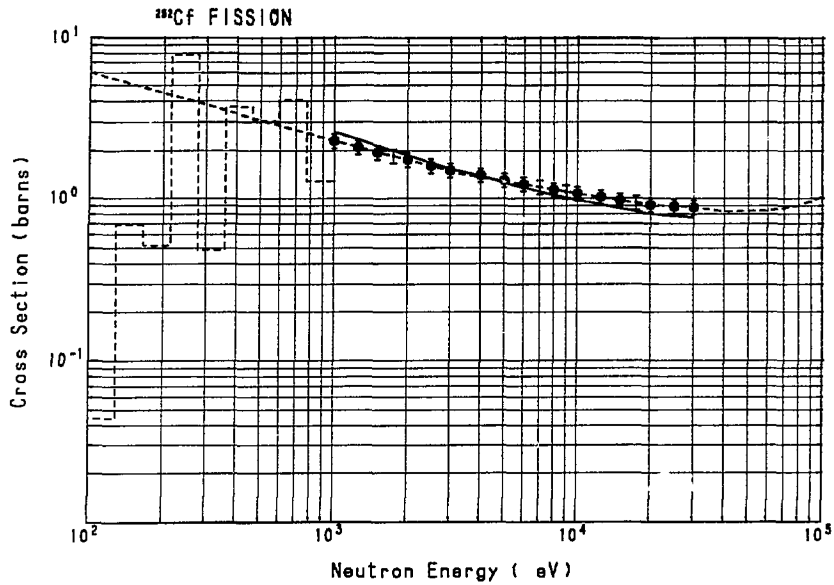

Fig. 3 Adjustment of unresolved resonance parameters to fission cross section. Solid curve is cross-section values calculated from the final parameters. Differences between the solid curve and circles which are cross sections to be reproduced were adopted as the background cross section

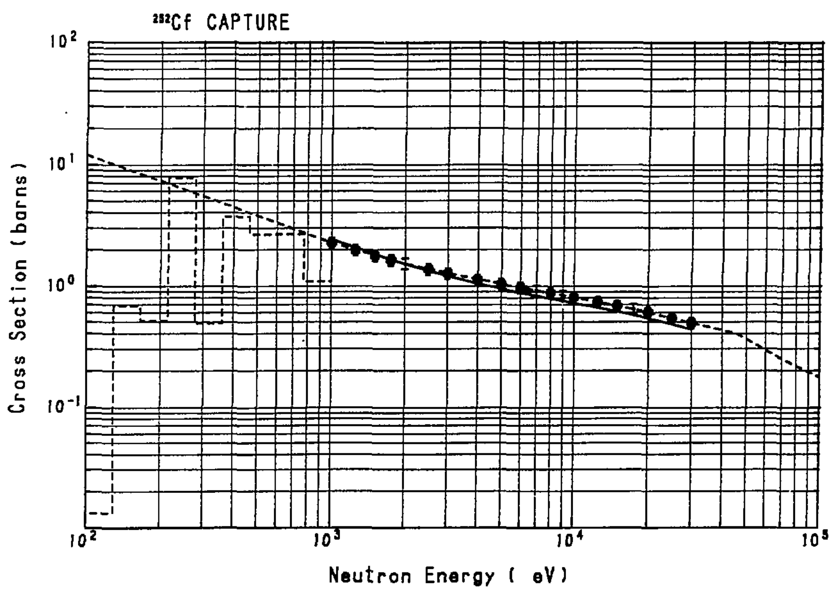

Fig. 4 Adjustment of unresolved resonance parameters to capture cross section

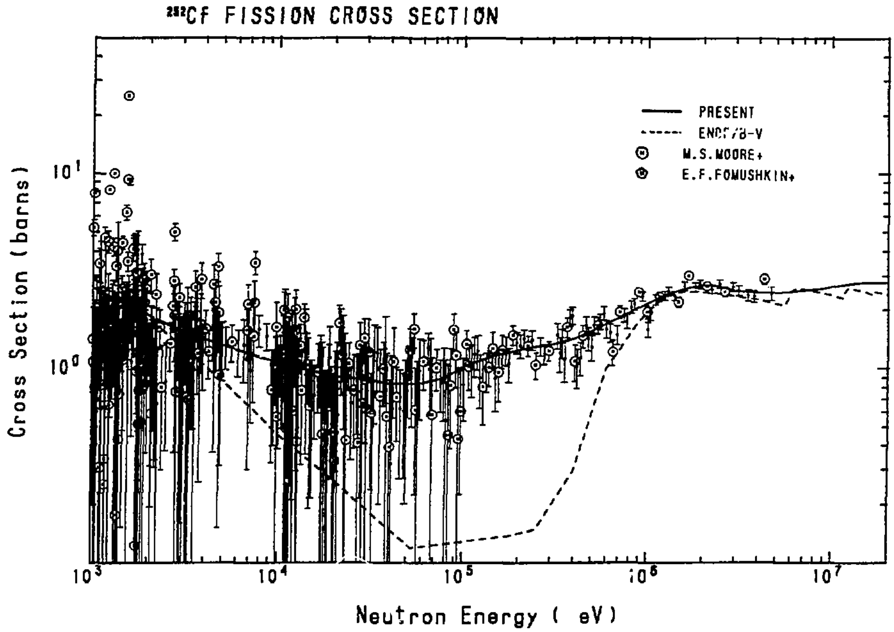

Fig. 5 ^{252}Cf Fission cross sections above 1.0 keV

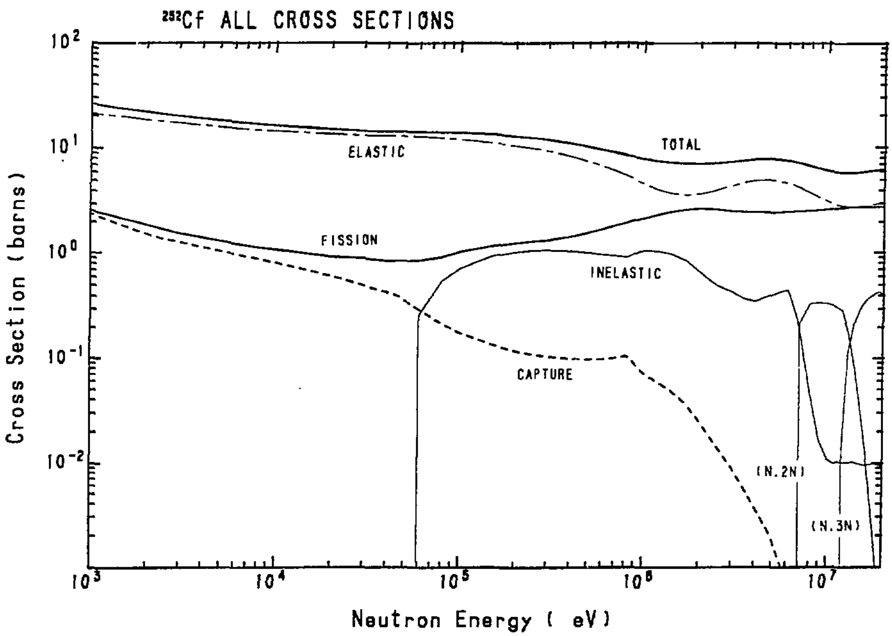

Fig. 6 All cross sections of ^{252}Cf

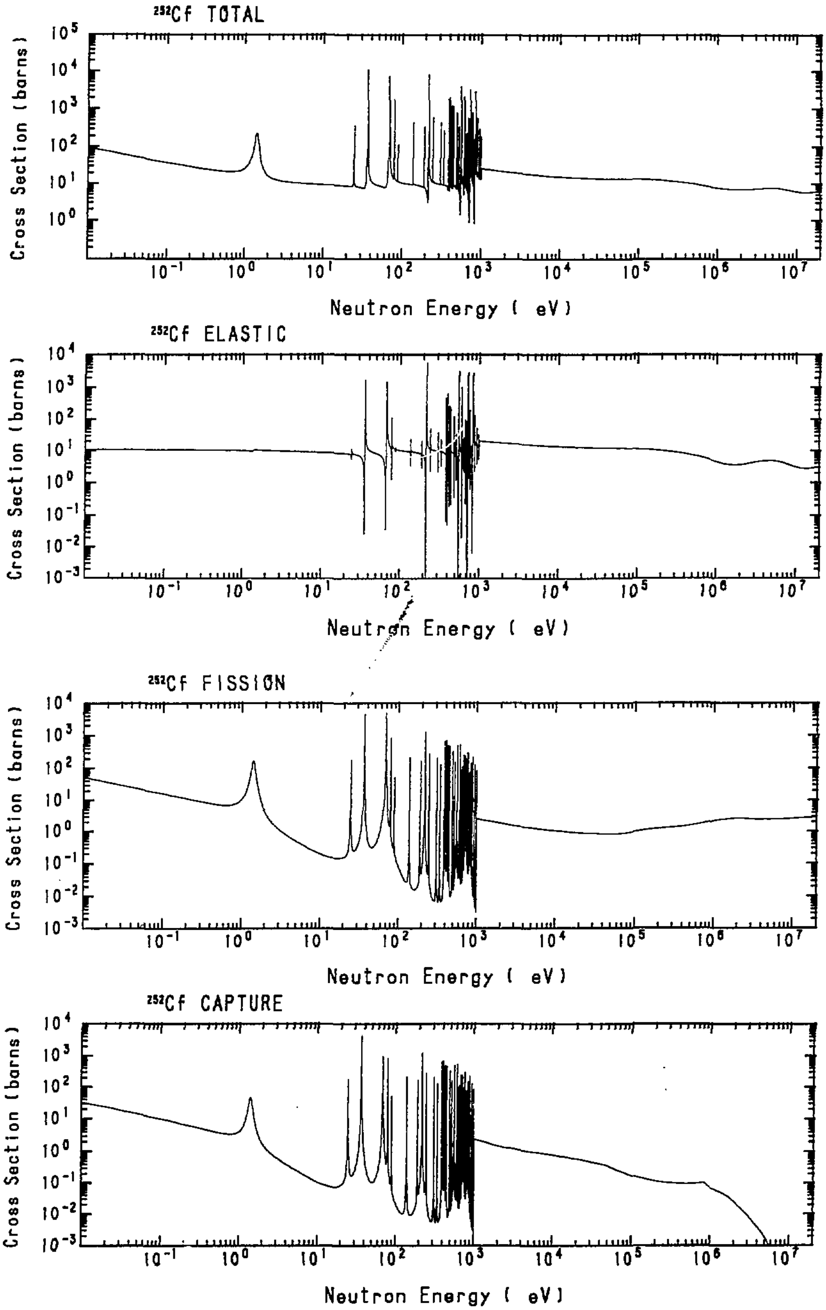

Fig. 7 Cross sections in the energy range from 0.01 eV to 20 MeV

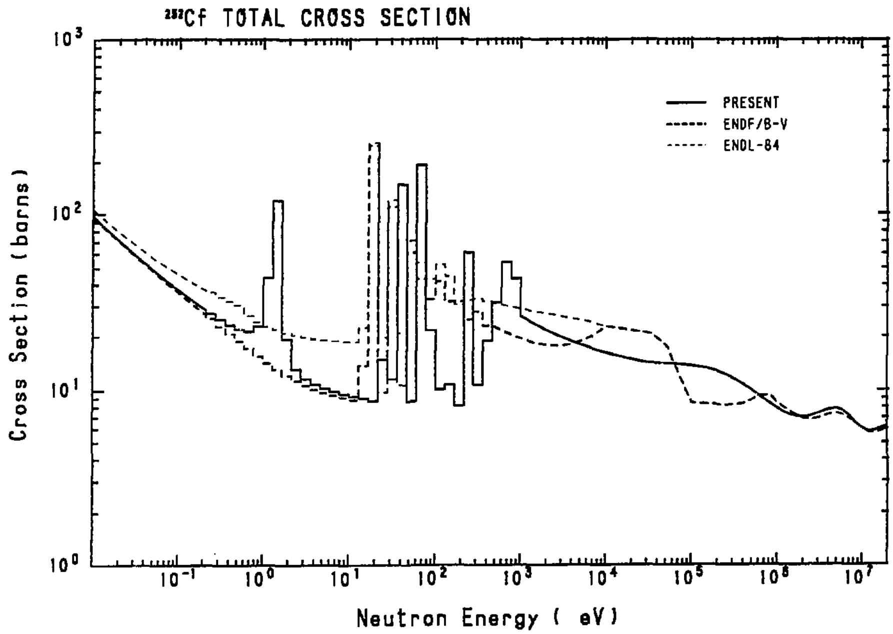

Fig. 8 Comparison of total cross sections

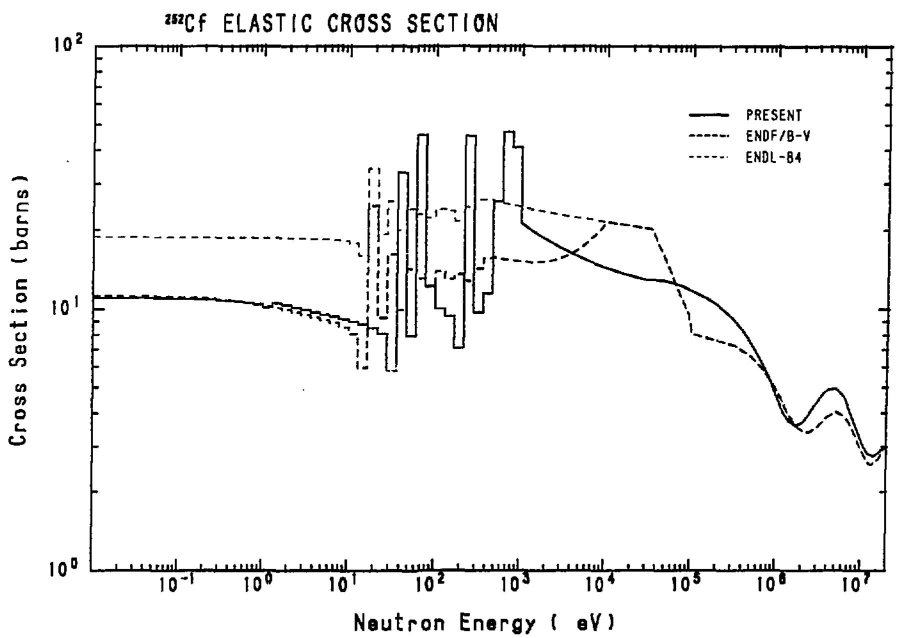

Fig. 9 Comparison of elastic scattering cross sections

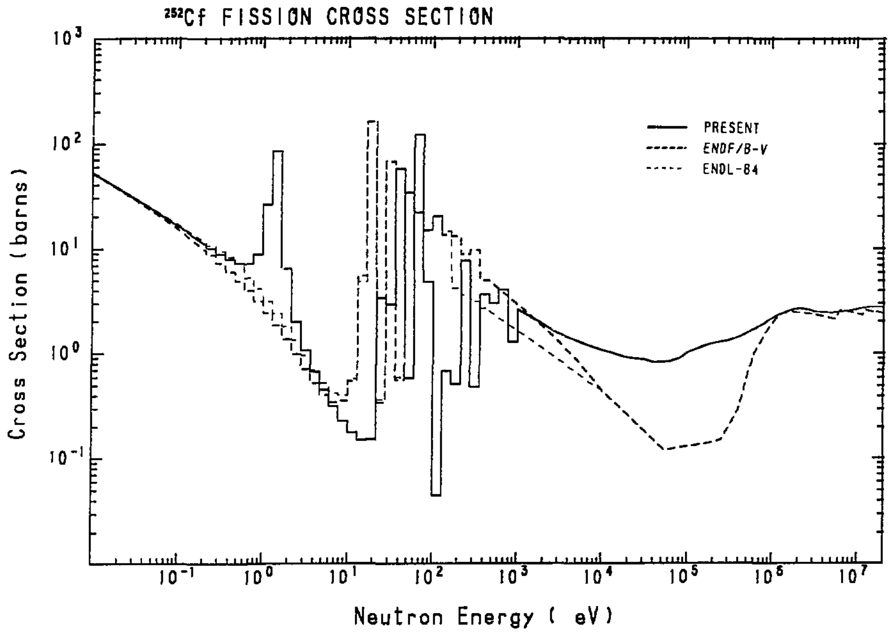

Fig. 10 Comparison of fission cross sections

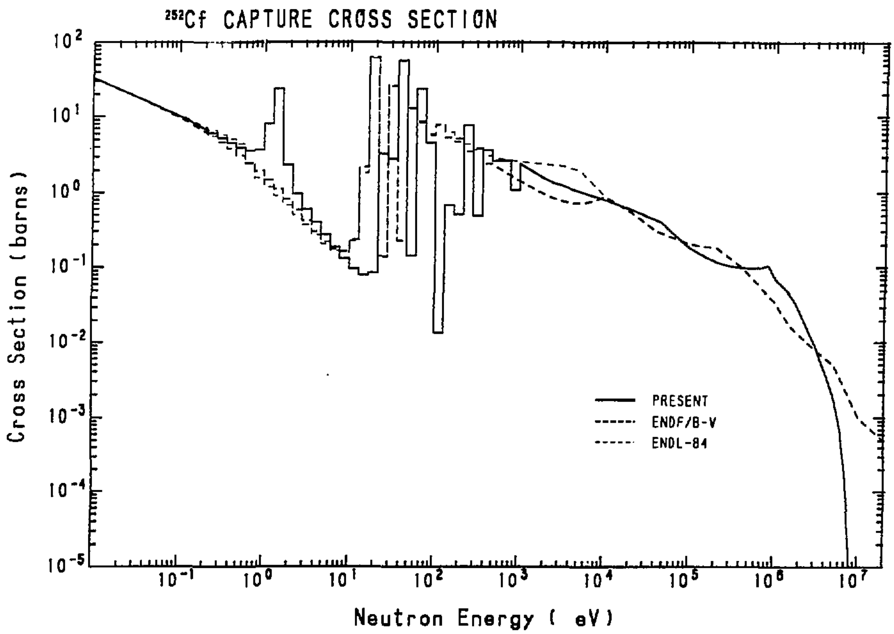

Fig. 11 Comparison of capture cross sections

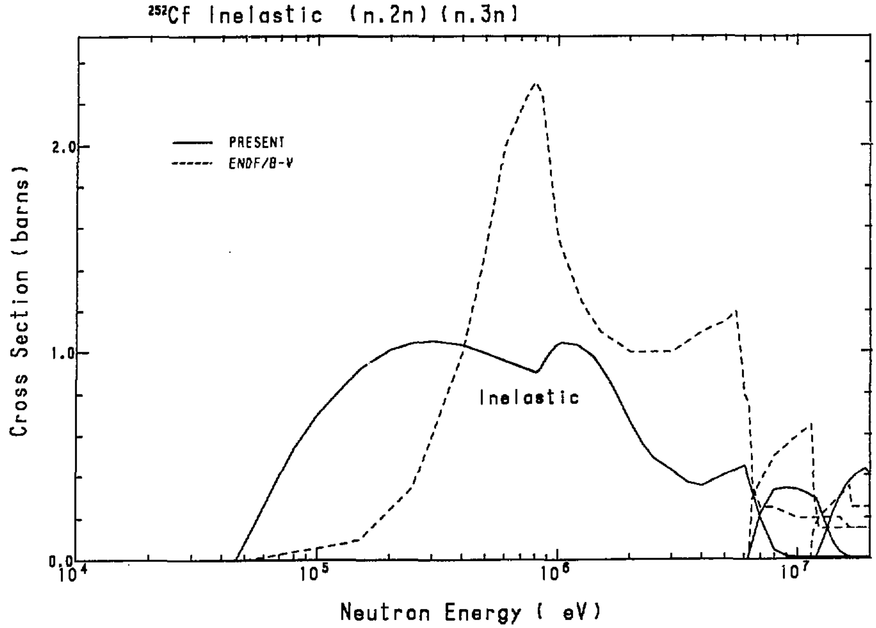

Fig. 12 Comparison of inelastic scattering, (n,2n) and (n,3n) cross sections

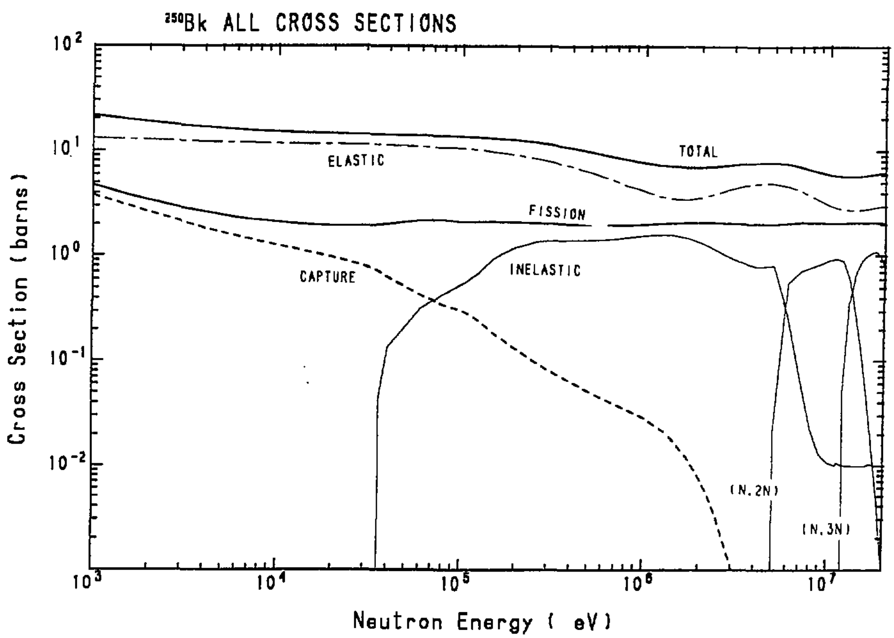

Fig. 13 All cross sections of ^{250}Bk

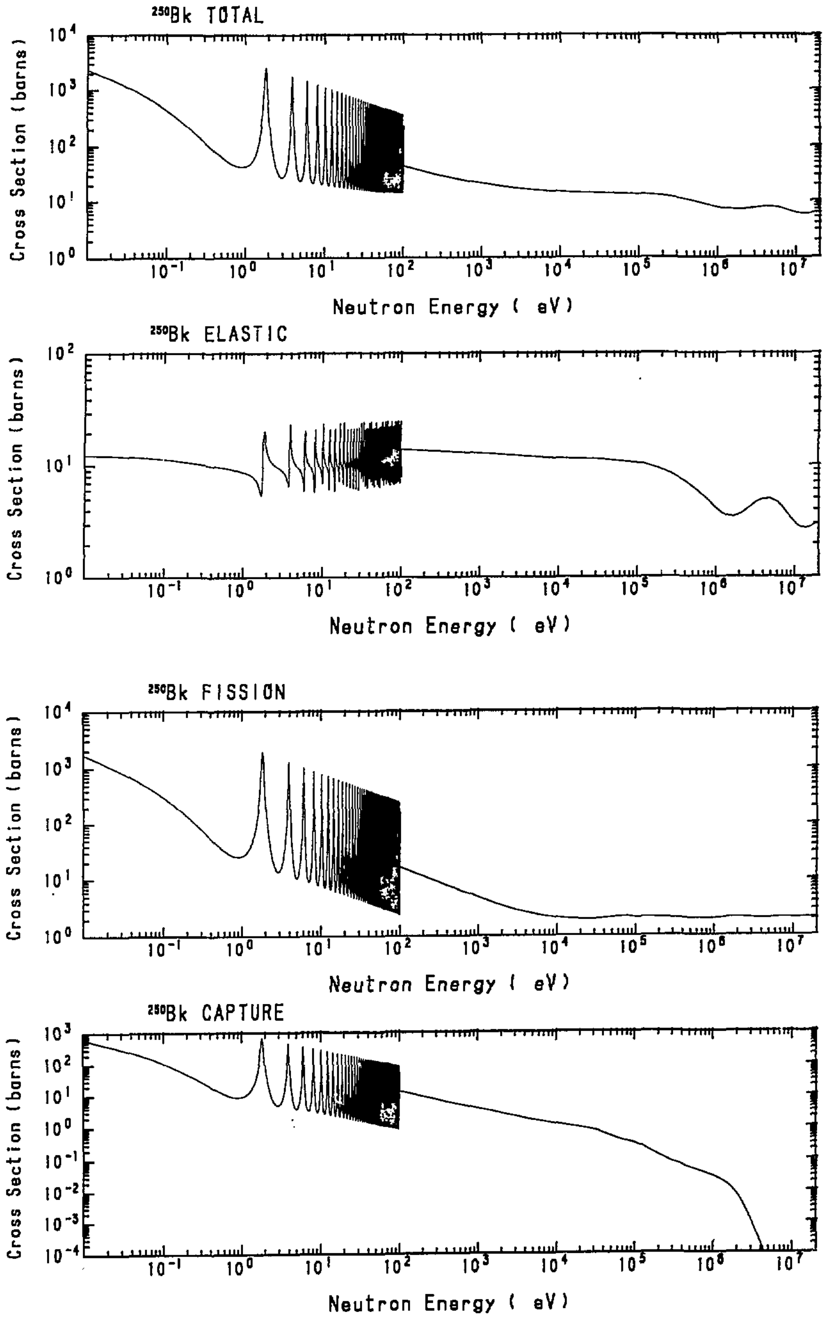

Fig. 14 Cross sections in the energy range from 0.01 eV to 20 MeV